Photoluminescence and optically detected magnetic resonance in a-Si:H/a-Si_3N_4:H multilayers

Masaaki Yamaguchi
Institute for Solid State Physics, University of Tokyo, Roppongi, Minato-ku, Tokyo 106, Japan

Kazuo Morigaki
Department of Electrical Engineering, Hiroshima Institute of Technology, Miyake, Saeki-ku, Hiroshima 731-51, Japan
(Received 11 April 1996)

The measurements of photoluminescence (PL) and optically detected magnetic resonance were carried out for a-Si:H/a-Si_3N_4:H multilayers. The results are accounted for in terms of the quantum-size effect. The alloy-effect model is also compared with the quantum-size-effect model for the interpretation of the results, particularly the temperature dependence of the PL intensity and the well-layer thickness (L_W) dependence of the PL efficiency. These results are also consistent with the quantum-size-effect model. The two-dimensional nature of recombination properties manifests itself for the multilayers with L_W of less than 30 Å. [S0163-1829(97)04304-X]

I. INTRODUCTION

Since the first fabrication of amorphous silicon-based multilayers by Abeles and Tiedje,[1] their electronic properties have been discussed in terms of the quantum-size effect. Recently, however, different interpretations based on the alloy effect have been proposed, for example, on the blueshift of the optical absorption edge associated with a decrease in the well-layer thickness of a a-Si:H/a-SiN_x:H multilayers.[2,3] In double-barrier structures based on a-Si:H and its alloy with nitrogen or carbon, observed bumplike irregularities in their current-voltage characteristics were first accounted for in terms of resonant tunneling.[4] Very recently, a doubt has been cast on this interpretation and another mechanism has been proposed, in which hopping conduction of carriers through the localized levels of the barrier layers is responsible for this phenomenon.[5] In any case, however, the authors have confirmed periodic multilayer structures in their samples.

In this paper, we present a detailed investigation on photoluminescence (PL) and optically detected magnetic resonance (ODMR) in a-Si:H/a-Si_3N_4:H multilayers. These measurements are greatly devoted to an understanding of the recombination processes and the nature of recombination centers in the multilayers. In Sec. II, we describe the preparation method for the multilayers and experimental procedures for PL and ODMR. We also show a photograph of periodic multilayer structures for the multilayer samples taken by a transmission electron microscope (TEM). In Sec. III, we present detailed results on PL and ODMR for multilayers as well as for bulk films of a-Si:H and a-$Si_{1-x}N_x$:H. In Sec. IV, we discuss the experimental results in terms of the quantum-size effect. We also comment on different interpretations based on the alloy effect. In Sec. V, conclusions are drawn.

II. EXPERIMENT

a-Si:H/a-Si_3N_4:H multilayers were prepared at 250 °C by using a capacitively coupled rf glow discharge system. SiH_4 diluted to 10% in H_2 was used to produce the a-Si:H well layers, and a gas mixture of SiH_4 (10% in H_2) and pure NH_3 having $\gamma \equiv [NH_3]/[SiH_4] = 10$ was used for the barrier layers of a-Si_3N_4:H (optical gap$\approx$5 eV). The flows of the two types of gas mixture were controlled by a microcomputer and were admitted to the reaction chamber alternately. Fused silica and/or crystal silicon were used as a substrate held on the grounded anode. The growth rate of the individual layers ranged from 0.6 to 1.3 Å/s and the residence time of gas in the reactor was about 1 s. During the interval between deposition of each layer, the system was evacuated and hence the rf plasma was interrupted. This interval time was 5 s. Further details for the correlation between the preparation conditions and the film quality have already been reported.[6] The characteristics of the samples used in this study are listed in Table I. The well-layer thickness L_W and barrier-layer thickness L_B range from 6 to 210 Å and from 5 to 75 Å, respectively. The barrier-layer thickness of 25 Å is sufficient for the confinement effect of photoexcited carriers, as will be seen from PL experiments concerning samples 5116, 5104, and 5106 mentioned in Sec. III A.

Periodic structures in our samples were evaluated by using x-ray diffraction and TEM. Sharp x-ray diffraction peaks were observed and showed the existence of well-defined superstructures. The layer spacing was determined from the Bragg diffraction angles, which was in good agreement with the layer thickness estimated from the deposition rate of the individual layer. The picture of the film cross section taken by JEOL-100U transmission electron microscope in Canon Research Center clearly showed the multilayer structure, as seen in Fig. 1. The optical gap was estimated from Tauc's plot of the absorption coefficient. The characteristics of the samples are also listed in Table I.

The steady-state PL experiments were carried out at 2–400 K, using unfocused Ar ion laser light of the photon energy $h\nu = 2.41$ eV (514.5 nm) and/or 2.54 eV (488 nm) and 0.2–500 mW (0.8–2000 mW/cm^2) for excitation chopped at about 80 Hz. The light intensity of 500 mW was used for the light-induced effects. The PL was dispersed with a single-prism monochromator to obtain the spectrum and was detected with a cooled germanium detector with a re-

TABLE I. Characteristics of samples. L_W, well-layer thickness; L_B, barrier-layer thickness.

Sample	L_W (Å)	L_B (Å)	Number of periods	Optical gap (eV)
		a-Si:H/a-Si_3N_4:H multilayers		
5103	6	25	350	2.36
5107	6	75	150	
5114	6	50	293	
5120	8	25	300	
5109	12	25	300	2.09
5115	12	50	201	
5104	18	25	250	2.00
5106	18	75	135	
5110	18	50	100	
5111	20	50	100	
5113	18	50	200	
5116	18	5	250	
5117	18	25	250	
5105	36	25	150	1.85
5112	72	25	100	
5121	210	25	36	
		a-Si:H		
1502	8400			≈1.80
		a-$Si_{1-x}N_x$:H		
2506	9000		$x=0.4$	2.40
2510	9200		$x=0.2$	2.18

sponse time of about 300 ns. The PL spectra were corrected for the spectral response of the detection system. The detection systems for PL and ODMR measurements were described in more detail in our previous paper.[7] For the electron spin resonance (ESR) measurements, an X-band JEOL spectrometer was used at room temperature.

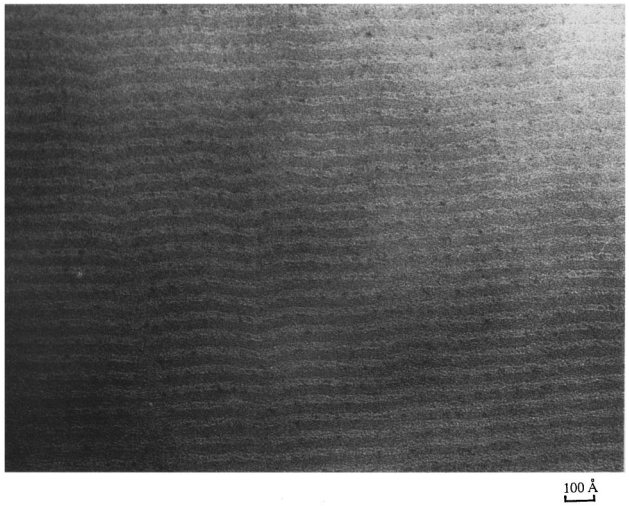

FIG. 1. Picture of the cross section of the a-Si:H/a-Si_3N_4:H multilayer film with $L_W=20$ Å and $L_B=50$ Å taken by a transmission electron microscope. It shows the periodic structure with L_W (a-Si:H)=20 Å and L_B (a-SiN:H)=50 Å.

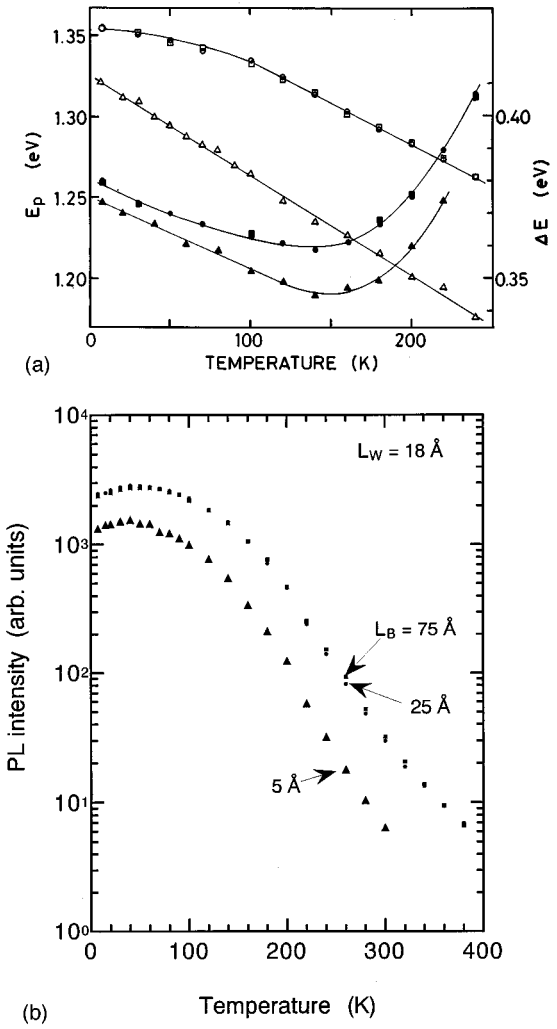

FIG. 2. Temperature dependence of (a) PL peak energy (open symbols) E_p and FWHM (solid symbols) ΔE, and (b) PL intensity at the peak energy in the steady-state PL spectra for a-Si:H/a-Si_3N_4:H multilayers with $L_W=18$ Å and $L_B=5$ Å (triangle), 25 Å (circle), and 75 Å (square). Excitation intensity for PL measurements is 20 mW.

III. RESULTS

A. L_B dependence of PL properties

First, in order to examine the effect of barrier-layer thickness L_B on PL properties such as the PL peak energy of PL spectrum E_p, the full width at half maximum (FWHM) ΔE, and the PL intensity at E_p, I_p, the temperature dependences of E_p, ΔE, and I_p in samples with $L_W=18$ Å and $L_B=5$, 25, and 75 Å have been measured as shown in Figs. 2(a) and 2(b), respectively. PL spectra of multilayers are shown in Fig. 3. Their behaviors in samples with $L_B=25$ and 75 Å are similar to each other and their values are almost the same. However, each value of the sample with $L_B=5$ Å is different from those of other samples.

Figure 4 shows the values of E_p, ΔE, and I_p at 7 K in samples with $L_W=18$ Å as a function of L_B. The values at $L_B=0$ Å are those of a-Si:H bulk film. E_p and I_p rapidly decrease and then increase through a minimum near $L_B=5$ Å and reach a constant value with increasing L_B. On the other hand, ΔE rapidly increases and reaches a constant

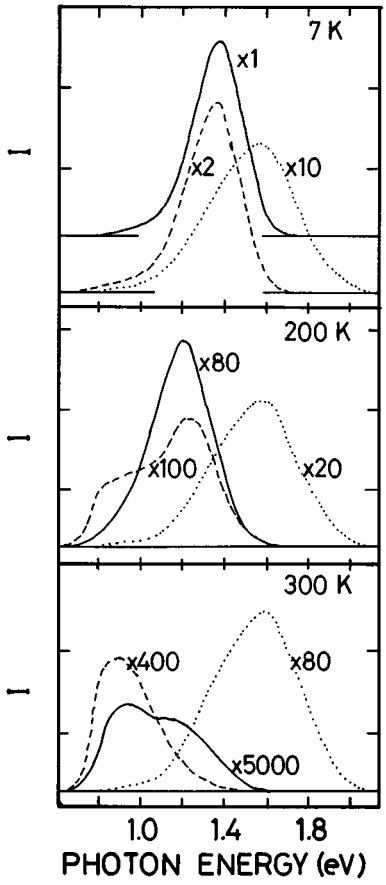

FIG. 3. Steady-state PL spectra measured at various temperatures such as 7, 200, and 300 K for a-Si:H bulk film (solid curves), a-Si:H/a-Si_3N_4:H multilayer film with $L_W=72$ Å and $L_B=25$ Å (broken curves), and that with $L_W=6$ Å and $L_B=25$ Å (dotted curves). Excitation intensity for PL measurements in 20 mW.

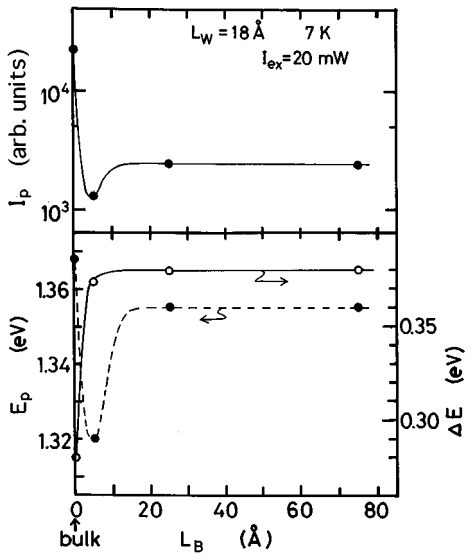

FIG. 4. PL peak energy E_p, FWHM ΔE, and PL intensity at the peak energy I_p at 7 K in samples with $L_W=18$ Å as functions of the barrier-layer thickness L_B. Excitation intensity I_{ex} for PL measurements is 20 mW.

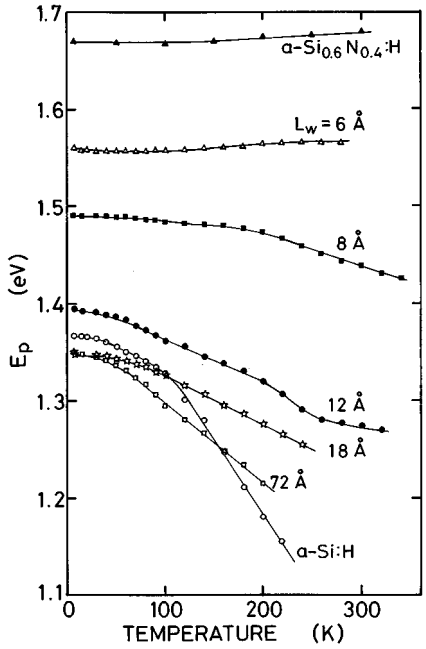

FIG. 5. Temperature dependences of the PL peak energy E_p in the steady-state PL spectra for a-Si:H, a-$Si_{0.6}N_{0.4}$:H, and a-Si:H/a-Si_3N_4:H multilayers with $L_B=25$ Å and various L_W.

value. These results suggest that PL properties are largely affected until $L_B=20$ Å, in other words, they are influenced by the interface region, which is estimated to be about 10 Å in thickness, and the nature of the interface region will be discussed in a separate paper.[8] Therefore, we consider that the value of $L_B=25$ Å is sufficient for the confinement effect of photoexcited carriers and we present the results of the samples with $L_B=25$ and/or 75 Å in the following.

B. Temperature dependence of PL spectra

The PL spectra observed at various temperatures in multilayers are shown in Fig. 3. With increasing the temperature from 7 K, two emission bands, i.e., the low-energy band (LEL) and the high-energy band (HEL) can be clearly observed, peaked at about 0.9 and 1.4 eV in a-Si:H and multilayers with rather thick L_W, e.g., in a multilayer with $L_W=72$ Å. The LEL is characterized by its weaker thermal quenching than the HEL.[6] Therefore, the LEL is most readily observed at high temperatures, as shown in Fig. 3. The peak intensity of the defect-related LEL at 300 K in a multilayer with $L_W=72$ Å is large by a factor of 20 compared with that in a-Si:H. This indicates that the radiative centers associated with the LEL are created at the interfaces between a-Si:H and a-Si_3N_4:H layers. Moreover, the LEL cannot be observed separately from the HEL as a well-defined band peaked at 0.9 eV with decreasing L_W down to 10 Å even at high temperatures.

The temperature dependences of E_p and ΔE in the PL spectra of multilayers and a-$Si_{0.6}N_{0.4}$:H are shown in Figs. 5 and 6, respectively. The shift of E_p toward lower energy in a-Si:H with increasing temperatures is partly due to a decrease in the energy band gap. Since E_p above 100 K in a-Si:H has a temperature coefficient of 1.53×10^{-3} eV/K in

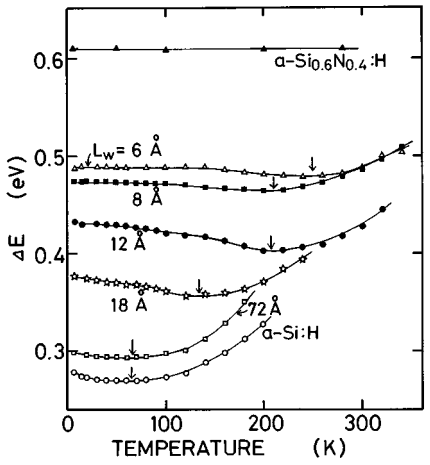

FIG. 6. Temperature dependences of FWHM, ΔE, in the steady-state PL spectra for a-Si:H, a-$Si_{0.6}N_{0.4}$:H, and a-Si:H/a-Si_3N_4:H multilayers with $L_B = 25$ Å, and various L_W. The arrows denote the temperature at which the value of FWHM shows the minimum.

comparison with a coefficient of 4.4×10^{-4} eV/K for the band gap,[9] the temperature dependence of E_p should be furthermore caused by another effect, i.e., the PL peak moves rapidly toward the red in a-Si:H, much faster than the gap, possibly due to thermalization of the photoexcited carriers down to the deep tail states.[10] The temperature coefficient of E_p for a-$Si_{1-x}N_x$:H alloy films and multilayers decreases with increasing the N content and decreasing L_W, respectively. A blueshift of E_p has been observed in the multilayer with $L_W = 6$ Å and a-$Si_{0.6}N_{0.4}$:H at temperatures above 150 K. In Fig. 6, ΔE decreases and then increases through a minimum with increasing temperatures. The temperature exhibiting the minimum of ΔE increases with decreasing L_W. These results will be discussed later.

Figure 7 shows the L_W dependence of E_p and ΔE associated with the main band at 7 and 200 K, as examples at the low and high temperatures, respectively. Optical gap E_g is also plotted as a function of L_W. E_p at 7 K gradually decreases and shows a minimum in spite of the increase in the optical gap and then rapidly increases when L_W decreases less than 20 Å. E_p at 200 K always increases with decreasing L_W. The redshift of E_p near $L_W = 40$ Å at 7 K is due to an increase in the PL intensity in the low-energy region, being associated with an increase in the density of the gap states created at the interfaces. A rapid broadening of ΔE is clearly observed with decreasing L_W, which is also associated with the increase of the tail states being due to the disorder caused by lowering of the effective dimension of L_W.

C. Temperature dependence of the PL intensity

The PL intensities at E_p, I_p, of the main emission band for various samples are shown as a function of temperature in Fig. 8. With increasing temperature from 7 K, a maximum of I_p observed around 50 K increases with increasing excitation density and decreasing the spin density of silicon dangling bonds, Si db, in a-Si:H.[9] We can also observe a maximum of I_p at about 50 K in all multilayers. However, we could not observe it in a-$Si_{0.6}N_{0.4}$:H. As will be discussed in Sec. IV, these results may be associated with the increase of

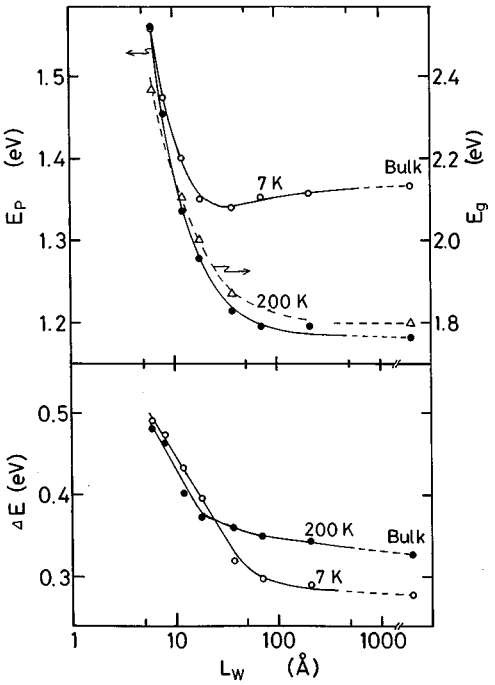

FIG. 7. L_W dependence of the PL peak energy E_p, FWHM ΔE, and the optical gap E_g (open triangle). Open and solid circles show the values measured at 7 and 200 K, respectively.

the generation rate of carriers caused by the confinement effect in the well layer and/or the decrease of the number of ''effective'' nonradiative centers in multilayers. It is also observed that the temperature dependence of I_p is weakened with decreasing L_W in multilayers and increasing the N content in a-$Si_{1-x}N_x$:H.

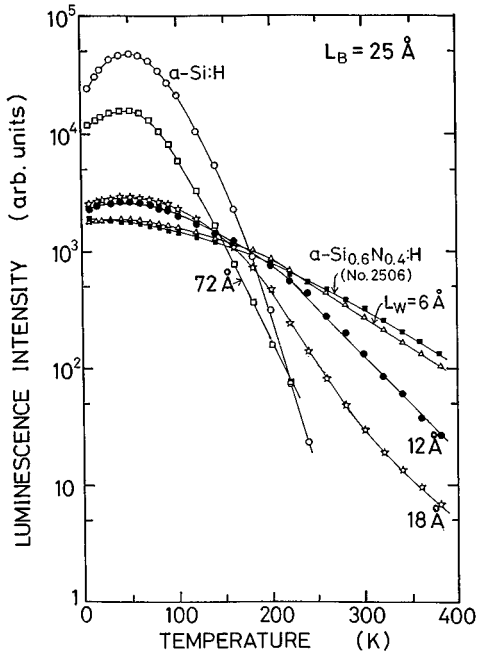

FIG. 8. Temperature dependences of the PL intensity at the peak energy associated with the main emission band for a-Si:H/a-Si_3N_4:H multilayers with $L_B = 25$ Å and various L_W and for bulk films of a-Si:H (sample 1502) and a-$Si_{0.6}N_{0.4}$:H (sample 2506).

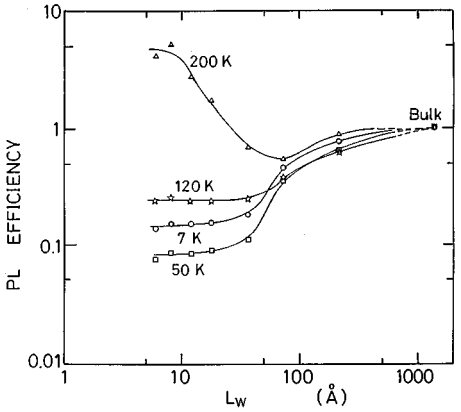

FIG. 9. PL efficiency as a function of L_W measured at various temperatures, normalized to the PL efficiency for a-Si:H at each temperature.

Figure 9 shows the PL efficiency, estimated from the PL spectra and normalized to that of a-Si:H for each temperature, as a function of L_W. At low temperatures such as 7, 50, and 120 K, the efficiency falls by about one order of magnitude compared with that for a-Si:H and tends to saturate with decreasing L_W. This behavior agrees with the similar results reported by other authors.[11,12]

D. ODMR signals in multilayers

In a-Si:H and a-$Si_{1-x}N_x$:H, the ODMR spectra generally consist of enhancing and quenching lines as have already been reported.[7,13–15] In a-Si:H films prepared at $T_s=250$ °C, we have observed asymmetric quenching and enhancing lines in which the quenching line shows FWHM≈19 G and is peaked at a g value of 2.0045 at $h\nu=1.44$ eV with a long tail toward lower magnetic field, while the enhancing line shows FWHM≈20 G and peaked at a g value of 2.0064 at $h\nu=0.8$ eV with a long tail toward lower magnetic field. In a-$Si_{1-x}N_x$:H films, both quenching and enhancing lines become symmetric with increasing the N content.

In the present experiment, we have observed a quenching $(-\Delta I)_{\rm ESR}$ and an enhancing signal $(\Delta I)_{\rm ESR}$, depending on excitation intensity $I_{\rm ex}$ and luminescence energy in multilayers; i.e., quenching lines are clearly observed at higher luminescence energy under weak $I_{\rm ex}$, while an enhancing line is dominantly observed under strong $I_{\rm ex}$, as observed in a-Si:H. The quenching and enhancing lines observed in multilayers with various L_W are shown in Fig. 10. We have observed the quenching line from the total PL under $I_{\rm ex}=0.5$ mW and the enhancing line at the PL energies of 0.88, 1.20, and 1.44 eV under $I_{\rm ex}=80$–500 mW. However, it should be noted that the sample with $L_W=6$ Å (samples 5103 and 5107) exhibits different behavior from other samples, namely, the enhancing line is not observed even at $I_{\rm ex}=100$ mW, but is observed at $I_{\rm ex}=500$ mW, as shown in Fig. 10. Both quenching and enhancing lines become symmetric with decreasing L_W. The g value, FWHM, and the value of $\Delta H_1/\Delta H_2, H_v$ in these lines are summarized as functions of L_W in Figs. 11(a) and 11(b), where H_v is taken as a measure of symmetry of the line shape as shown in the

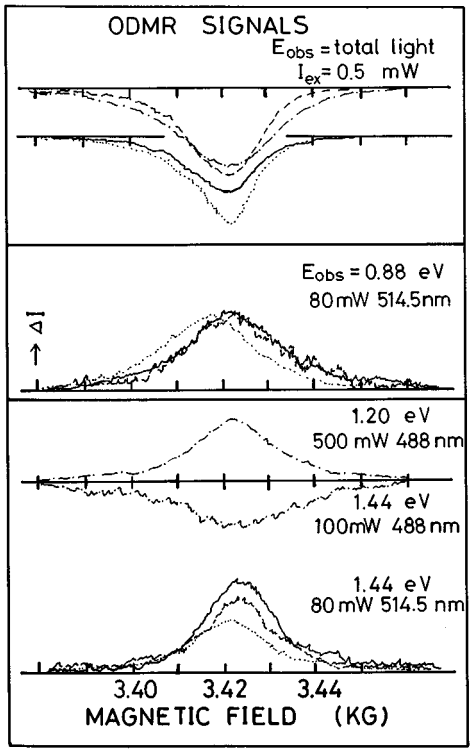

FIG. 10. Quenching and enhancing signals for a-Si:H/a-Si_3N_4:H multilayers with $L_B=25$ or 75 Å and various L_W, i.e., $L_W=6$ Å (dashed-dotted curves, samples 5103 and/or 5107), 12 Å (broken curves, sample 5109), 18 Å (solid curves, sample 5106), and 36 Å (dotted curves, sample 5105). $I_{\rm ex}$ and $E_{\rm obs}$ denote the excitation intensity and photon energy at which ODMR signals were observed, respectively.

figure. The open and solid circles show each value before and after prolonged illumination ($I_{\rm ex}=500$ mW for 30 min), respectively. The g value of the quenching line is almost constant as a function of L_W, i.e., $g\approx2.0045$ as shown in Fig. 11(a). After prolonged illumination, the g value remains unchanged within the experimental error, so its results are not shown in Fig. 11(a). FWHM decreases slightly from that of a-Si:H film and then increases with decreasing L_W. H_v gradually decreases from $H_v=1.9$ in a-Si:H and then rapidly approaches $H_v=1$ with decreasing L_W from $L_W=20$ Å. This indicates that the signal becomes symmetric in the multilayers with decreasing L_W. We consider the reason for the symmetry of the signal in the following.

The quenching line in a-Si:H is composed of three lines with g-values of 2.004, 2.01, and 2.005, which are associated with trapped electrons at positively charged threefold-coordinated Si atoms, T_3^+ centers, trapped holes at negatively charged threefold-coordinated Si atoms, T_3^- centers, and Si-db, respectively, as was discussed before.[16] If the creation of the negative U centers such as T_3^+ and T_3^- centers in a-Si:H of the well layer is suppressed by the influence of the barrier layer of a-Si_3N_4:H, the unresolved quenching lines with $g\approx2.004$ and 2.01, designated by the light-induced ESR (LESR) lines, disappear and the quenching line due to Si db can be only observed in multilayers with small L_W. Concerning the g value of multilayers with small L_W, i.e., $g=2.0045$, its deviation from that of a-Si:H

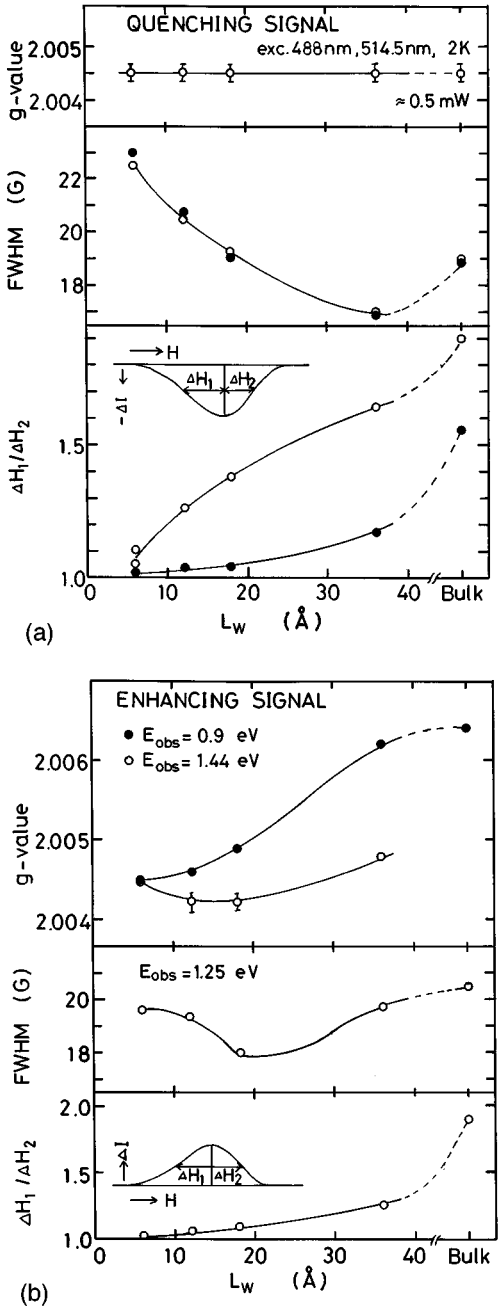

FIG. 11. g value, FWHM, and $\Delta H_1/\Delta H_2$ for (a) quenching and (b) enhancing signals as functions of L_W.

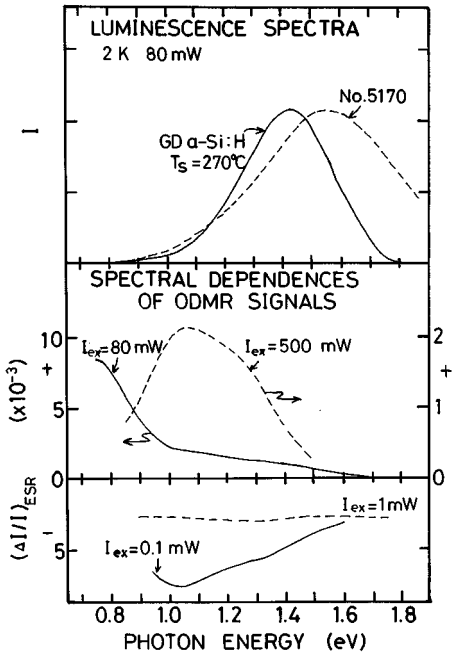

FIG. 12. PL spectra and spectral dependence of enhancing and quenching signals in a-Si:H prepared at 270 °C (solid curves) and a-Si:H/a-Si_3N_4:H multilayer with $L_W=6$ Å (broken curves). PL intensities are plotted in arbitrary units.

($g=2.0055$) partially originates from the increase in the band-gap energy. The g value of multilayers with large L_W corresponds to the peak of the overlapped three lines mentioned above. The results for the FWHM are also accounted for in terms of the above model. With decreasing L_W, the FWHM decreases, owing to the decrease of the number of negative U centers. This results in the approach of $H_v=1$. The line broadening of Si db resonance for small L_W is related to the variation of band-gap energy due to spatial fluctuations of L_W in the multilayer. A significant broadening with decreasing from $L_W=30$ Å may correspond to a rapid increase in the band-gap energy of the multilayer. After prolonged illumination, the signal becomes more symmetric than before prolonged illumination, because the number of Si db's increases;[17] i.e., the quenching signal is mainly due to Si db. In a-Si:H bulk film, the quenching lines corresponding to the LESR centers were not enhanced after prolonged illumination at low temperatures such as 2 K.[18] This behavior is also seen in the multilayer films of the present concern, as shown in Fig. 11(a). These are the reasons for a different L_W dependence of H_v before and after prolonged illumination, as shown in Fig. 11(a). The light-induced effects will be reported in a separate paper.[8]

Figure 11(b) shows the g value, FWHM, and H_v of the enhancing line as a function of L_W. The enhancing line, particularly before illumination, in a-Si:H is due to the self-trapped holes in specific weak Si-Si bonds, i.e., a weak Si-Si bond adjacent to an Si-H bond (the so-called A center)[13,15,16,19] and its spectral dependences of ODMR signals is shown in Fig. 12. The g value of the enhancing line has a spectral dependence, as reported before.[14] The g values of the enhancing lines measured at $h\nu=0.9$ eV (solid circles) and 1.44 eV (open circles) are presented as functions of L_W as an example, although those are measured at several $h\nu$. With decreasing L_W, the g value in the low luminescence energy region ($h\nu=0.9$ eV) rapidly decreases, while the g values in the high luminescence energy region ($h\nu=1.44$ eV) are almost constant, i.e., the spectral dependence of the g value becomes small. The FWHM decreases slightly and then increases and the shape of the line becomes symmetric with decreasing L_W. It has been considered that the enhancing line measured before illumination in a-Si:H is caused by one radiative center, the A center, in spite of its asymmetric line shape; i.e., the A center is anisotropic in nature. With decreasing L_W, the spectral dependences of the g value in the enhancing line become small and the anisotropy of the A center presumably disappears because of the

multilayer structure. Therefore, the enhancing line concerning the A center becomes symmetric and therefore this results in narrowing of the line; i.e., the FWHM becomes small. With further decreasing L_W such as to $L_W = 6$ Å, only the N-related radiative center, i.e., the E center,[14] has been observed, namely, the observed enhancing line with $g \approx 2.0045$ at 0.9 and 1.44 eV is due to the E center and the enhancing line due to the A center is observed only for samples with $L_W \geq 12$ Å in Fig. 11(b), as will be mentioned below. The spectral dependence of the ODMR signal due to the E center (broken curves) is also shown in Fig. 12. This line is symmetric and its FWHM is about 20 G. These considerations are also suggested by the spectral dependences of ODMR signals and the excitation intensity dependences of ODMR signals, as will be described in a separate paper,[8] and are also confirmed by those of photoinduced absorption in multilayers, i.e., the holes in the valence-band tail are not self-trapped but are distributed with a Gaussian function in the valence-band tail for multilayers with $L_W < 10$ Å.[20,21]

IV. DISCUSSIONS

A. General aspects of recombination in the multilayer films

Electrons and holes created by band-to-band excitation are confined in the well layers, so that their recombination with each other is enhanced compared to in bulk films. When the well layer becomes thin, recombination is becoming two-dimensional in nature. The confinement effect and two-dimensional recombination mentioned above have already been suggested from the time-resolved PL and ODMR measurements in a-Si:H/a-$Si_{1-x}N_x$:H multilayer films.[22] The initial decay of the PL intensity just after a pulsed laser light excitation is turned off becomes rapid with decreasing L_W. The confinement effect of electrons and holes results in a rapid thermalization of electrons into the conduction band tail and also in an increase of the density of trapped electrons and holes. The multilayer film with $L_W = 6$ Å exhibits a slow decay of the PL intensity after the initial rapid decay in contrast with those with $L_W = 12$ and 18 Å which show similar decay to a-Si:H bulk films. This is accounted for in terms of the two-dimensional feature of nonradiative recombination via Si db's, namely the recombination probability of electrons and holes at Si db's is significantly reduced when L_W becomes small compared to the average separation of Si db's. The above features of recombination in the multilayer films are also observed in the present PL and ODMR experiments.

B. PL and ODMR properties

In order to interpret the results mentioned in Sec. III, we consider a model for the recombination properties of photoexcited carriers in multilayers. According to previous experiments in a-Si:H (Refs. 7 and 23) that is the material of the well layer in multilayers, HEL arises from radiative recombination between tail electrons and self-trapped holes, i.e., A centers, at low temperatures and between tail electrons and tail holes at higher temperatures, where self-trapping of holes becomes unstable. LEL has been identified as due to radiative recombination of trapped electrons in defects, E centers, with trapped holes mentioned above. Si db's, T_3^0, and positively and negatively charged threefold-coordinated Si (negative U), i.e., T_3^+ and T_3^-, act as nonradiative centers. A possible model for the E centers is the separate T_3^+-N_2^- pair defects in order to account for the behaviors of LEL and ODMR,[7] where N_2^- is the negatively charged twofold-coordinated nitrogen. In a-$Si_{1-x}N_x$:H, that is the material of the barrier layer in multilayers, the situations for the recombination properties are almost the same as those in a-Si:H except for the addition of the E^* centers, which are newly introduced to explain the results of light-induced effects in a-$Si_{1-x}N_x$:H.[14] E^* centers are the trapped electron centers being composed of close T_3^+-N_2^- pairs and act as nonradiative centers. Therefore, E^* centers are readily created by the existence of many Si db's and N atoms in a-SiN:H with a high content of hydrogen and the strong lattice distortion may occur around the E^* center. In multilayers, i.e., when both a-Si:H and a-SiN:H layers contact each other, electrons flow from the a-SiN:H layer into the a-Si:H layer, because of the difference in the work function of each layer material.[24] As a result, some of Si db's, T_3^0, in the a-Si:H layer become T_3^- (positive U), while some of Si db's in the a-SiN:H layer becomes T_3^+ (positive U). Thus, as twofold-coordinated nitrogen N_2^0 seems to be present in the a-SiN:H layer, coupled pairs T_3^+-N_2^- are considered to be formed in the interface region. When T_3^+ and N_2^- are separated with each other, this pair defect (E center) contributes to LEL and to the enhancing signal, while close T_3^+-N_2^- pairs (E^* centers) seem to us to contribute to nonradiative recombination in a similar way to the case of a-$Si_{1-x}N_x$:H.

There are several interesting features concerning PL and ODMR results in multilayers. First, we take the blueshift of E_p and the narrowing of ΔE with increasing temperatures, as shown in Figs. 5 and 6. Those are phenomenologically due to the fact that the thermal quenching of the PL band is not uniform over all photon energy. First we consider the PL spectra of a-Si:H presented in Fig. 13. The upper figure shows the PL spectra for various temperatures in a-Si:H. For comparison among PL spectra at various temperatures, the spectra are normalized at the PL peak intensity and plotted on a logarithmic scale, as shown in the lower figure. The high-energy part of the spectrum quenches more rapidly than the low-energy part with increasing temperatures. This results in a decrease in E_p, as shown in Fig. 5. Another remarkable feature in the PL spectra is that the normalized PL in the low-energy region at 50 K also quenches, compared with that at 7 K. This results in the minimum of ΔE; i.e., the narrowing of the PL spectra occurs at a certain temperature. This is also the case for the multilayer, in which the temperature exhibiting a minimum of ΔE increases with decreasing L_W, as shown by an arrow in Fig. 6. On the other hand, the PL spectra of the a-$Si_{0.6}N_{0.4}$:H alloy film are almost independent of temperature. These results are associated with the redistribution of the carriers trapped in the conduction- and valence-band tail after photoexcitation and therefore greatly depends on the temperature and the width of tail states, i.e., in general, as the temperature increases, shallow tail electrons are thermally reexcited into the conduction band, so that the demarcation level distinguishing between trapping and recombination goes down and consequently E_p shifts towards lower energy. In the case of the sample with the

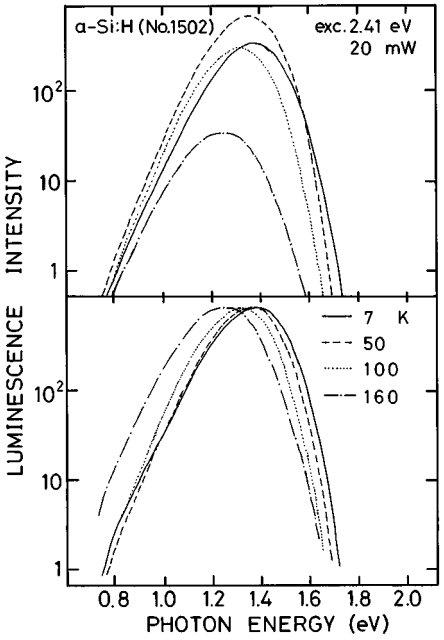

FIG. 13. PL spectra measured at various temperatures under $I_{ex}=20$ mW for a-Si:H (the upper figure) and PL spectra normalized at the PL peak intensity (the lower figure).

wide width of the conduction-band tail, photogenerated electrons are thermalized into deep levels in the conduction-band tail, so that the photogenerated electrons thermally reexcited to the conduction band decrease in number. They nonradiatively recombine with trapped holes via nonradiative centers such as Si db's. In this case, the nonradiative recombination mainly occurs by their tunneling to a defect even at high temperatures. As a result, the weak temperature dependence of PL intensity is observed in the sample with wide tail states as shown in Fig. 8. The decrease and increase in ΔE with temperature are caused by lowering of the demarcation level, redistribution of trapped electrons in the band tail, and a crossover from self-trapped holes to tail holes distributed over the valence-band tail states. The blueshift of E_p observed only in the sample with wide tail states is due to the redistribution of carriers by their hopping at higher temperatures.

Next we discuss the thermal quenching of I_p observed above 50 K in terms of reexcitation of trapped electrons in the conduction-band tail. I_p in the temperature region where the thermal quenching is observed is given by

$$I_p = I_0/[1 + A\ \exp(T/T_0)], \tag{1}$$

where I_0 is the I_p in the low-temperature limit, and T_0 and A are constants.[9] This relationship can be postulated on the assumption that thermally excited carriers in extended states diffuse away to nonradiative sites and that the density of localized states below the mobility edge varies as $\exp(-E/E_0)$. Here, E is the depth taken from the conduction-band edge and E_0 is a constant, corresponding to the width of the band tail states. The relationship between T_0 and E_0 can be expressed by the relationship[9]

$$T_0 = E_0/k\ \ln(\omega_0 \tau_R), \tag{2}$$

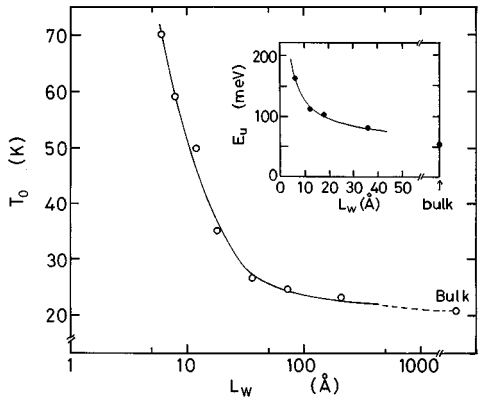

FIG. 14. Plot of T_0 as a function of L_W. The inset shows the Urbach tail width E_u as a function of L_W.

where k, ω_0, and τ_R are the Boltzmann constant, the attempts to escape frequency, and radiative decay time, respectively. We obtain the value of T_0 from the slope of the linear relationship between $(I_0/I_p)^{-1}$ and $\exp(T/T_0)$. The value of T_0 obtained is shown as a function of L_W in Fig. 14. The relationship between E_u and L_W is also shown in the inset of Fig. 14, where E_u is the characteristic width of the Urbach tail, which is measured from the photothermal deflection spectroscopy (PDS) at room temperature.[25] However, in our model, the measured values of T_0 are related to the width E_0 of the conduction-band tail, while that of E_u corresponds to the width of the valence-band tail. T_0 varies with L_W in a similar way to E_u. The conduction-band tail is broadened with decreasing L_W, so that the temperature variation on I_p becomes gentle in a similar way to that for a-$Si_{0.6}N_{0.4}$:H whose band tail is also broad. This shows that the temperature dependence of I_p can be interpreted in terms of the thermal quenching model mentioned above.

We have considered the reason why PL intensity shows the peak around 50 K on the basis of the PL decay curves.[26] At low temperatures such as 7 K, photogenerated electron-hole pairs with the long recombination lifetime, ≈ 50 ms, exist. However, with increasing temperature the number of these pairs decreases and redistribution of carriers easily occurs; i.e., some electrons thermalized into deep tail states are reexcited thermally into shallower tail states having large radiative recombination rates via hopping. Then, this causes the PL intensity to increase.

Next, we consider the PL efficiency as a function of L_W in Fig. 9. At low temperatures the electrons trapped in the conduction-band tail cannot be excited thermally to the extended states and recombine with trapped holes radiatively or nonradiatively via the defects. Therefore, the decrease in η is closely related to the density of nonradiative centers N_s and η is given by the expression[27]

$$\eta = \exp(-4\pi R_c^3 N_s/3) \tag{3}$$

by assuming that the band tail electrons and holes in a-Si:H are sufficiently immobile at low temperatures so that nonradiative recombination occurs by their tunneling to a defect, where the critical distance R_c is defined as that for which nonradiative tunneling becomes more probable than radiative tunneling within the electron-hole pair. According

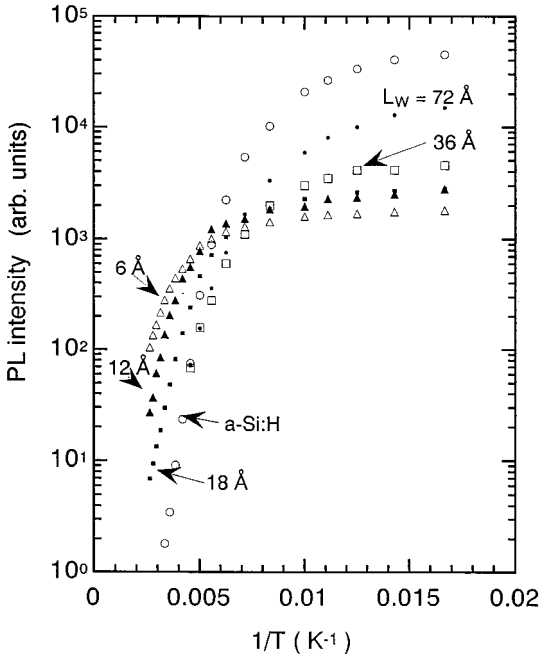

FIG. 15. PL intensity plotted against T^{-1} for a-Si:H/a-Si_3N_4:H multilayers with $L_W=6$ Å (open triangle, $E_{th}=0.15$ eV), 12 Å (solid triangle, $E_{th}=0.19$ eV), 18 Å (solid square, $E_{th}=0.20$ eV), 36 Å (solid square), and a-Si:H bulk film (open circle, $E_{th}=0.26$ eV).

to PDS (Ref. 25) and ESR (Ref. 28) measurements, the number of defects per unit volume within the well layer becomes large with decreasing L_W. When L_W becomes small compared with the average separation of defects, the recombination probability of electrons and holes at the defect is significantly reduced.[22] This is due to the two-dimensional feature of nonradiative recombination via defects. In this case, η is given by

$$\eta=\exp(-\pi R_c^2 L_W N_s). \tag{4}$$

From this relationship, the saturation of η in multilayers with less than $L_W=30$ Å such as shown in Fig. 9 suggests that the product of L_W and N_s in Eq. (4) may be nearly constant. The observed variation of N_s with L_W by our recent ESR measurement[28] shows this behavior instead of the three-dimensional feature given by Eq. (3) for multilayers with L_W of less than 30 Å.

Since the thermal quenching effect is weakened for multilayers with small L_W and the nonradiative recombination via tunneling is almost independent of temperature, the electron-hole confinement effect manifests itself in multilayers with thin well layers at higher temperatures such as 200 K.

We have considered the temperature variation of I_p in terms of the thermal quenching of PL. Here, however, we point out that the temperature variation of I_p has also been discussed in terms of a model of self-trapping of holes, namely, there is a crossover from self-trapped holes to tail holes distributed over the valence-band tail states around 140 K with increasing temperature.[23] This manifests itself in part in the activated behavior of the temperature variation of I_p, as shown in Fig. 15. The activation energy E_{th} measured from the slope of the $\ln I_p$ versus $1/T$ curve corresponds to either an average thermal excitation energy of tail electrons particularly in PL or the thermal depth of the self-trapped hole level. The values for each sample are given in the caption of Fig. 15. The value of 0.26 eV for a bulk a-Si:H sample almost corresponds to the latter value, while those for multilayer films may correspond to the former value.

The ODMR signal consists of quenching and enhancing signals. The quenching signal is mainly due to Si db's, as described above. It is suggested from the spectral dependence of ODMR signals that two radiative centers exist near $g\approx 2.0$ in multilayers. One is the self-trapped hole center, the A center, and the other is the E center. This identification is consistent with the result of the L_W dependence of the g value of the enhancing lines shown in Fig. 11(b). As mentioned in Sec. III, g value of the enhancing line, A line, observed at 0.9 eV decreases with decreasing L_W, while that of the enhancing line, E line, observed at 1.44 eV exhibits a different behavior from that observed at 0.9 eV, namely, a small change with L_W. A decrease of the g value at 0.9 eV with L_W is associated with an increase in the band gap. On the other hand, another enhancing line, the E line, has been attributed to an electron trapped at a T_3^+-N_2^- pair defect, which exist preferentially in the interface region, particularly on the barrier-layer side. Thus, they are hardly affected by the well layer, namely, the quantum-size effect. As a result, their g value does not exhibit a significant change with L_W. For $L_W=6$ Å, the observed enhancing line is only due to the E center. We think that the A center is not observed in the multilayer with $L_W=6$ Å as has already been suggested.[17] These results coincide with those of the photo-induced absorption;[20] i.e., the A center is observed for the multilayer with $L_W\geq 10$ Å, while for $L_W<10$ Å, the A center becomes unstable and thus holes are trapped in the valence-band tail, because the lattice relaxation probably may not occur for holes to be self-trapped in specific Si-Si bonds of the a-Si:H well layer being sandwiched by a-Si_3N_4:H barrier layers with the stronger bond strength.

C. Comparison of the quantum-size effect model with the alloy model

In the following, we compare the PL properties of the a-Si:H/a-Si_3N_4:H multilayers with those of a-SiN:H alloys. An increase of I_p is observed around 50 K in all multilayers (see Fig. 8). As mentioned before, this is observed by increasing the excitation intensity and/or decreasing the spin density of Si db's in a-Si:H; i.e., the increase of the photoexcited carrier density. However, we could not observe it in a-$Si_{1-x}N_x$:H samples 2506 ($E_g=2.40$ eV) and 2510 ($E_g=2.18$ eV). These are caused by the difference in the nonradiative recombination properties between multilayers and a-SiN:H, i.e., the recombination properties in multilayers are mainly associated with the a-Si:H well layer and the interface region. In other words, this is due to the increase of the photoexcited carrier density caused by the confinement effect of photogenerated carriers in a-Si:H well layer.

As has already been pointed out, η at low temperatures shows a constant value below $L_W\approx 30$ Å and this indicates that nonradiative recombination of two-dimensional nature operates in the well layer with L_W of less than 30 Å, as

shown in Eq. (4). If the alloying effect operates at the interface, the N content in the a-Si:H well layer increases with decreasing L_W. If so, and the two-dimensional nature of nonradiative recombination is neglected, η should decrease with decreasing L_W because of the increase of the Si db's density associated with the increase in the N content in a-Si:H, but this is not the case, as seen in Fig. 9. Therefore, this result is considered to be due to the recombination process in the multilayer structure, as was discussed in detail concerning the result of Fig. 9.

The PL decay behavior in bulk films and multilayers is also consistent with a model of the quantum-size effect. A detailed account of the PL decays will be reported elsewhere.

V. CONCLUSION

We conclude that the results of the PL and ODMR measurements for a-Si:H/a-Si_3N_4:H multilayers are consistent with a model of the quantum-size effect. A model of the alloy effect was examined for comparison, particularly for the temperature dependence of the PL intensity and the dependence of the PL efficiency on L_W. These results suggest that the two-dimensional nature of the recombination properties plays an important role in the PL intensity and the PL efficiency for the multilayers with L_W of less than 30 Å. This allows us to conclude that the quantum-size effect has been observed for such multilayers having thin well layers.

ACKNOWLEDGMENTS

We wish to thank Dr. T. Nakagiri, Dr. S. Kato, and A. Ishizaki, Canon Research Center, for taking the TEM picture of the multilayer film. This picture was originally published in Kotai Butsuri[29] to whose publisher we acknowledge for courtesy of reproduction of Fig. 1 in this paper.

[1] B. Abeles and T. Tiedje, Phys. Rev. Lett. **51**, 2003 (1983).
[2] M. Beaudoin, C. J. Arsenault, and M. Meunier, J. Non-Cryst. Solids **137&138**, 1099 (1991).
[3] N. Bernhard, H. Dittrich, and G. H. Bauer, J. Non-Cryst. Solids **137&138**, 1103 (1991).
[4] S. Miyazaki, Y. Ihara, and M. Hirose, Phys. Rev. Lett. **59**, 125 (1987).
[5] N. Bernhard, B. Frank, B. Movaghar, and G. H. Bauer, Philos. Mag. B **70**, 1139 (1994).
[6] M. Yamaguchi, H. Ohta, C. Ogihara, and K. Morigaki, Mater. Sci. Eng. B **5**, 385 (1990).
[7] M. Yamaguchi, K. Morigaki, and S. Nitta, J. Phys. Soc. Jpn. **58**, 3828 (1989).
[8] M. Yamaguchi and K. Morigaki, Phys. Rev. B (to be published).
[9] R. A. Street, Adv. Phys. 30, 593 (1981), and references therein.
[10] R. A. Street, in *Semiconductors and Semimetals*, Vol. 21B, edited by J. I. Pankove (Academic Press, Orlando, 1984), p. 197.
[11] P. G. LeComber, W. E. Spear, R. A. Gibson, M. Hopkinson, P. K. Bhat, M. Searle, and I. G. Austin, J. Non-Cryst. Solids **77&78**, 1081 (1985).
[12] W. C. Wang and H. Fritzsche, J. Non-Cryst. Solids **97&98**, 919 (1987).
[13] K. Morigaki, in *Semiconductors and Semimetals*, Vol. 21C, edited by J. I. Pankove (Academic Press, Orlando, 1984), p. 155.
[14] M. Yamaguchi, K. Morigaki, and S. Nitta, J. Phys. Soc. Jpn. **60**, 1769 (1991).
[15] K. Morigaki and M. Kondo, Solid State Phen. **44–46**, 731 (1995).
[16] K. Morigaki and M. Yoshida, Philos. Mag. B **52**, 289 (1985).
[17] M. Yamaguchi and K. Morigaki, J. Non-Cryst. Solids **137&138**, 1135 (1991).
[18] D. Han, M. Yoshida, and K. Morigaki, Solid State Commun. **63**, 1083 (1987).
[19] K. Morigaki, H. Hikita, and M. Kondo, J. Non-Cryst. Solids **190**, 38 (1995).
[20] H. Ohta, M. Yamaguchi, C. Ogihara, and K. Morigaki, Solid State Commun. **66**, 797 (1988).
[21] H. Ohta and K. Morigaki, Philos. Mag. **60**, 153 (1989).
[22] C. Ogihara and K. Morigaki, J. Phys. Soc. Jpn. **57**, 4409 (1988).
[23] K. Morigaki, M. Yamaguchi, and I. Hirabayashi, J. Non-Cryst. Solids **164–166**, 571 (1993).
[24] J. Robertson and M. J. Powell, J. Non-Cryst. Solids **77&78**, 1007 (1985).
[25] K. Yatabe, H. Ohta, M. Yamaguchi, and K. Morigaki, Philos. Mag. **60**, 73 (1989).
[26] M. Yamaguchi and K. Morigaki, Philos. Mag. **60**, 127 (1989).
[27] C. Tsang and R. A. Street, Philos. Mag. B **37**, 601 (1978).
[28] K. Morigaki, Y. Fujita, and M. Yamaguchi (unpublished).
[29] K. Morigaki and Kotai Butsuri, Solid State Phys. **27**, 851 (1992).